Article

Mechanism of Product Release in NO Detoxification from *Mycobacterium tuberculosis* Truncated Hemoglobin N

Marcelo A. Mart, Axel Bidon-Chanal, Alejandro Crespo, Syun-Ru Yeh, Victor Guallar, F. Javier Luque, and Daro A. Estrin

J. Am. Chem. Soc., **2008**, 130 (5), 1688-1693 • DOI: 10.1021/ja076853+

J|A|C|S
ARTICLES
Published on Web 01/12/2008

Mechanism of Product Release in NO Detoxification from *Mycobacterium tuberculosis* Truncated Hemoglobin N

Marcelo A. Martí,[†] Axel Bidon-Chanal,[‡] Alejandro Crespo,[†] Syun-Ru Yeh,[§] Victor Guallar,*[,||] F. Javier Luque,*[,‡] and Darío A. Estrin*[,†]

Departamento de Química Inorgánica,Analítica y Química Física/INQUIMAE-CONICET, Facultad de Ciencias Exactas y Naturales, Universidad de Buenos Aires, Ciudad Universitaria, Pabellón 2, Buenos Aires, C1428EHA, Argentina, Departament de Fisicoquímica and Institut de Biomedicina (IBUB), Facultat de Farmàcia, Universitat de Barcelona, Av. Diagonal 643, 08028, Barcelona, Spain, Department of Physiology and Biophysics, Albert Einstein College of Medicine of Yeshiva University, Bronx, New York 10461, and ICREA, Computacional Biology Program, Barcelona Supercomputing Center, Edificio Nexos II, Barcelona 08028, Spain

Received September 10, 2007; E-mail: dario@qi.fcen.uba.ar; fjluque@ub.edu; victor.guallar@bsc.es

Abstract: The capability of *Mycobacterium tuberculosis* to rest in latency in the infected organism appears to be related to the disposal of detoxification mechanisms, which converts the nitric oxide (NO) produced by macrophages during the initial growth infection stage into a nitrate anion. Such a reaction appears to be associated with the truncated hemoglobin N (trHbN). Even though previous experimental and theoretical studies have examined the pathways used by NO and O_2 to access the heme cavity, the eggression pathway of the nitrate anion is still a challenging question. In this work we present results obtained by means of classical and quantum chemistry simulations that show that trHbN is able to release rapidly the nitrate anion using an eggression pathway other than those used for the entry of both O_2 and NO and that its release is promoted by hydration of the heme cavity. These results provide a detailed understanding of the molecular basis of the NO detoxification mechanism used by trHbN to guarantee an efficient NO detoxification and thus warrant survival of the microorganism under stress conditions.

Introduction

About one-third of the human population is infected by *Mycobacterium tuberculosis*.[1] During the initial growth infection stage, nitric oxide (NO) produced by macrophages contributes to restricting the bacteria in latency.[2,3] However, NO detoxification mechanisms have evolved in several pathogenic microorganisms to reduce the potential damage produced by the nitrosative stress. In *M. tuberculosis* such a mechanism appears to consist of the oxidation of NO with heme-bound O_2 to yield the harmless nitrate ion (eq 1),[4−6] a reaction associated with the truncated hemoglobin N (trHbN).

$$\mathrm{Fe(II)O_2 + NO \rightarrow Fe(III) + NO_3^-} \qquad (1)$$

The trHbN pertains to a distinct group within the globin superfamily[7] and folds following a 2-on-2 helical sandwich motif instead of the 3-on-3 one of the classical globin fold.[8] The proximal HisF8 heme-linked residue is conserved in both Hb and trHb families, but a distal tyrosine at position B10, which contributes to modulating the oxygen affinity, is found in almost all the trHb family members sequenced to date.[9] Another relevant feature of trHbN from *M. tuberculosis* is that it displays a structurally conserved apolar tunnel system that connects the heme pocket with the protein surface, which consists of two perpendicular branches of about 8 and 20 Å in length, respectively.[10,11]

Experimental studies demonstrated that the NO-dioxygenase activity in trHbN is limited by the rate of ligand diffusion to the heme cavity,[4,5] which stimulated a variety of studies to identify the role of the tunnel in ligand migration. Previous studies suggested that the protein matrix tunnel follows a ligand-induced dynamical regulation mechanism,[12−14] where (i) O_2 and NO would access the heme cavity through the short and long

[†] Universidad de Buenos Aires.
[‡] Universitat de Barcelona.
[§] Albert Einstein College of Medicine of Yeshiva University.
[||] Barcelona Supercomputing Center.

(1) Bloom, B. R. *Tuberculosis: Pathogenesis, Protection and Control*; ASM Press: Washington, DC, 1994.
(2) MacMicking, J. D.; North, R. J.; LaCourse, R.; Mudgett, J. S.; Shah, S. K.; Nathan, C. F. *Proc. Natl. Acad. Sci. U.S.A.* **1997**, *94*, 5243.
(3) Shiloh, M. U.; Nathan, C. F. *Curr. Opin. Microbiol.* **2000**, *3*, 35.
(4) Couture, M.; Yeh, S. R.; Wittenberg, B. A.; Wittenberg, J. B.; Ouellet, Y.; Rousseau, D. L.; Guertin, M. *Proc. Natl. Acad. Sci. U.S.A.* **1999**, *96*, 11223.
(5) Ouellet, H.; Ouellet, Y.; Richard, C.; Labarre, M.; Wittenberg, B.; Wittenberg, J.; Guertin, M. *Proc. Natl. Acad. Sci. U.S.A.* **2002**, *99*, 5902.
(6) Pathania, R.; Navani, N. K.; Gardner, A. M.; Gardner, P. R.; Dikshit, K. L. *Mol. Microbiol.* **2002**, *45*, 1303.
(7) Moens, L.; Vanfleteren, J.; van de Peer, Y.; Peeters, K.; Kapp, O.; Czeluzniak, J.; Goodman, M.; Blaxter, M.; Vinogradov, S. *Mol. Biol. Evol.* **1996**, *13*, 324.
(8) Pesce, A.; Couture, M.; Dewilde, S.; Guertin, M.; Yamauchi, K.; Ascenzi, P.; Moens, L.; Bolognesi, M. *EMBO J.* **2000**, *19*, 2424.
(9) Milani, M.; Pesce, A.; Nardini, M.; Ouellet, H.; Ouellet, Y.; Dewilde, S.; Bocedi, A.; Ascenzi, P.; Guertin, M.; Moens, L.; Friedman, J. M.; Wittenberg, J. B.; Bolognesi, M. *J. Inorg. Biochem.* **2005**, *99*, 97.
(10) Milani, M.; Pesce, A.; Ouellet, Y.; Ascenzi, P.; Guertin, M.; Bolognesi, M. *EMBO J.* **2001**, *20*, 3902.
(11) Milani, M.; Pesce, A.; Ouellet, Y.; Dewilde, S.; Friedman, J. M.; Ascenzi, P.; Guertin, M.; Bolognesi, M. *J. Biol. Chem.* **2004**, *279*, 21520.
(12) Crespo, A.; Martí, M. A.; Kalko, S. G.; Morreale, A.; Orozco, M.; Gelpí, J. L.; Luque, F. J.; Estrin, D. A. *J. Am. Chem. Soc.* **2005**, *127*, 4433.

 10.1021/ja076853+ CCC: $40.75

branches of the tunnel, respectively, and (ii) opening of the long branch is promoted upon O_2 binding to the heme through a local conformational change in the TyrB10-GlnE11 pair, which acts as a molecular switch that triggers a global change in the dynamical behavior of the protein. Accordingly, it can be speculated that such a regulation mechanism has evolved to optimize the efficiency of the O_2/NO chemistry, as the access of NO to the heme cavity should take place only upon binding of O_2 to the heme.

In this work the eggression pathway followed by the nitrate anion is examined by means of electronic structure, hybrid quantum mechanical−molecular mechanical, and classical molecular dynamics simulations. The critical role of trHbN as a NO-detoxifying enzyme demands that the nitrate anion formed in the heme cavity must be released efficiently to the aqueous solvent to enable the protein to start a new enzymatic cycle. However, the high hydrophobic character of the two branches of the tunnel makes it difficult to conceive that the nitrate anion might leave the heme cavity through the tunnel system. The results reveal that the nitrate anion is released rapidly through a distinct eggression pathway, which is not delineated in the X-ray crystallographic structure of the oxygenated form of trHbN.

Computational Methods

Classical Simulations. Molecular dynamics (MD) simulations were performed starting from the optimized trHbN·NO_3^- complex obtained in our previous work,[12] which in turn was based on the X-ray crystallographic structure of the oxygenated form of trHbN (PDB entry 1idr; chain A at 1.9 Å resolution). The enzyme was immersed in a preequilibrated octahedral box of TIP3P[15] water molecules. The final system contained the protein and around 8600 water molecules (ca. 28270 atoms). Simulations were performed in the NPT ensemble. The system was simulated employing periodic boundary conditions and Ewald sums for treating long-range electrostatic interactions (with the default Amber-9 parameters). All simulations were performed with the parmm99 force field of the Amber-9 package.[16] The atomic charges for the heme group were derived using the protocol reported in our previous works.[12] For the nitrate anion, charges of −0.437 *e* and 0.311 *e* were assigned to O and N atoms. For the heme-bound nitrate anion, the main differences in the partial charges concerned the oxygen atom linked to iron and the nitrogen atom, whose effect is attenuated by the restrain imposed to the Fe−O bond, but similar charges were obtained for the external oxygens. Finally, the Lennard−Jones parameters were taken from those assigned to negatively charged oxygen (similar to carboxylate oxygen) and sp^2 nitrogen.

The free energy profile for migration of the nitrate anion was determined by means of multiple steered molecular dynamics (MSMD) simulations. The free energy was obtained using Jarzynski's inequality.[17] The chosen reaction coordinate only pulls the nitrate anion from the heme active site, without imposing any constraint to a predefined eggression pathway. The free energy profile was built up by combining two independent free energy profile calculations which included 10 independent MSMD runs each.

Mixed Quantum Mechanics/Molecular Mechanics (QM/MM) Methods. QM/MM calculations were carried out with the QSite program.[18] Geometry optimizations were carried out using the B3LYP functional[19] in combination with the LACVP* and LACV3P* basis sets.[20] A frozen orbital was chosen at the QM/MM boundary, and classical mechanics were described with the AA-OPLS2001 force field.[21] A detailed description of the QM/MM methods and protocols can be found in previous studies.[22] The initial model for the QM/MM calculation was taken from a representative snapshot taken from the classical MD trajectory. Since the QM/MM protocol uses energy minimization, all water molecules beyond 10 Å from the protein surface were removed, and all water oxygen atoms beyond 6 Å from the protein surface were frozen in geometry minimizations and reaction coordinate computations. QM calculations were performed with the Jaguar program[23] using the same functional and basis set.

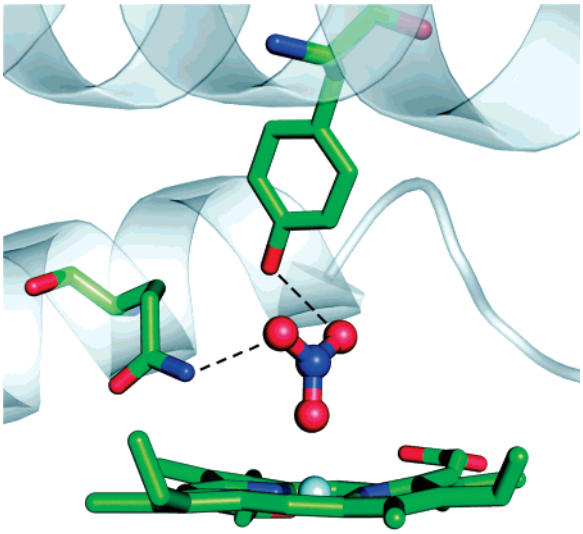

Figure 1. Representation of selected residues in the active site of the truncated hemoglobin N from *M. tuberculosis* for the state corresponding to the heme group bound to the nitrate anion. The hydrogen-bond interactions of the nitrate anion with TyrB10 and GlnE11 are shown by dashed lines.

Results and Discussion

The release of the nitrate anion to the aqueous environment can be limited by two processes: (i) the breaking of the bond between the anion and the heme group or (ii) the diffusion of the anion through the protein matrix. It can be anticipated that the former process will be penalized not only by the loss of the interaction energy between the anion and the Fe(III) atom but also by the loss of hydrogen-bond contacts with TyrB10 and GlnE11 (Figure 1).[12] On the other hand, though hydration by the bulk solvent can be conceived to be the driving force for the release of the anion, migration through the protein cannot be easily envisaged due to the hydrophobic character of the protein matrix tunnel, unless a distinct pathway mediates eggression of the anion. Under these circumstances, the release of the nitrate anion to the bulk solvent might be too slow, which could limit the efficiency of the NO detoxification mechanism associated with trHbN and therefore the survival of the microoganism. On the basis of these considerations, it is reasonable to expect that the protein has evolved an eggression

(13) Bidon-Chanal, A.; Martí, M. A.; Crespo, A.; Milani, M.; Orozco, M.; Bolognesi, M.; Luque, F. J.; Estrin, D. A. *Proteins* **2006**, *64*, 457.
(14) Bidon-Chanal, A.; Martí, M. A.; Estrin, D. A.; Luque, F. J. *J. Am. Chem. Soc.* **2007**, *129*, 6782.
(15) Jorgensen, W. L.; Chandrasekhar, J.; Madura, J. D.; Impey, R. W.; Klein, M. L. *J. Chem. Phys.* **1983**, *79*, 926.
(16) Pearlman, D. A.; Case, D. A.; Caldwell, J. W.; Ross, W. R.; Cheatham, T. E., III; DeBolt, S.; Ferguson, D.; Seibel, G.; Kollman, P. *Comp. Phys. Commun.* **1995**, *91*, 1.
(17) Jarzynski, C. *Phys. Rev. Lett.* **1997**, *78*, 2690.
(18) *Qsite*, 4.0; Schrodinger, LLC: New York, 2005.
(19) (a) Becke, A. D. *Phys. Rev. A* **1988**, *38*, 3098. (b) Lee, C.; Yang, W.; Parr, R. G. *Phys. Rev. B* **1988**, *37*, 785.
(20) Hay, P. J.; Wadt, W. R. *J. Chem. Phys.* **1985**, 82, 270.
(21) Kaminski, G. A.; Friesner, R. A.; Tirado-Rives, J.; Jorgensen, W. L. *J. Phys. Chem. B* **2001**, *105*, 6474.
(22) Friesner, R. A.; Guallar, V. *Annu. Rev. Phys. Chem.* **2005**, *56*, 389.
(23) *Jaguar*, 6.5; Schrodinger, LLC: New York, 2005.

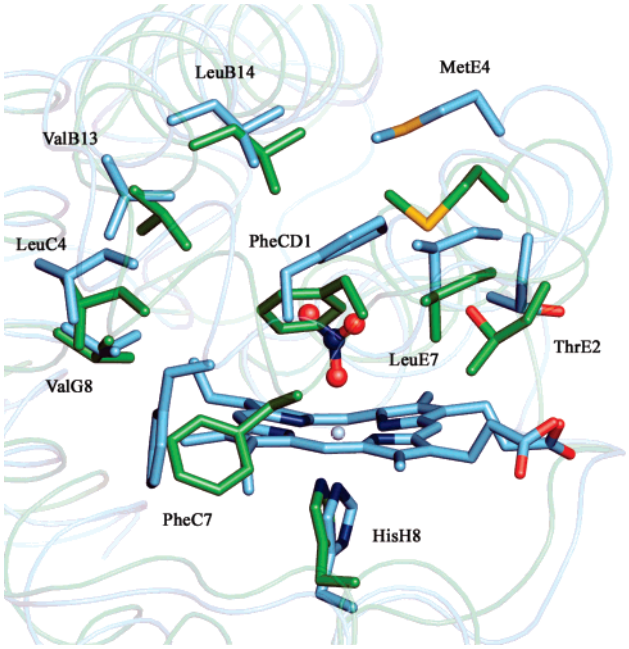

Figure 2. Representation of the average position adopted by selected residues at the heme cavity obtained upon superposition of representative structures of the wild type trHbN.O_2 protein (green) and the protein with heme-bound nitrate anion (blue).

mechanism to ensure an efficient turnover, which in turn should rely on the weakening of the interaction between Fe(III) and nitrate anion, and the delineation of an efficient eggression pathway from the heme cavity to the aqueous environment.

MD Simulation of the Nitrate-Anion-Bonded Protein. It might be hypothesized that the presence of the negative charge in the product formed from the reaction between the heme-bound O_2 and NO might disturb the structure of the cavity walls and eventually give rise to structural changes that facilitate the breaking of the bond between the heme group and the nitrate anion. To check this hypothesis, a 30 ns MD simulation of trHbN with a heme-bound nitrate anion was run. A stable trajectory was obtained with rmsd values for the backbone of the core residues (16−127) around 1.6 Å (see Figure S1 in the Supporting Information). The residues 32−58, which form the cavity walls, are the main contributors to the rmsd (by excluding these residues, the rmsd decreases to 1.2 Å).

Compared to O_2, the larger size of the nitrate anion and its negative charge induce a significant local rearrangement of residues TyrB10, ValB13, LeuB14, PheC7, PheCD1, MetE4, and LeuE7, which are pushed between 0.5 and 1.5 Å far away from the Fe atom relative to their position in the wild type trHbN oxygenated protein. As a result, the heme cavity is enlarged by a factor of ca. 2, as determined from the average volumes of the heme cavities measured[24] for a set of 50 snapshots taken randomly in the final part of the trajectory and from the simulation corresponding to the wild type trHbN oxygenated protein[14] (Figure 2).

Due to the conformational rearrangement, the compactness of the cavity walls is notably reduced, which facilitates the entry of water molecules to the interior of the cavity. Two distinct pathways by which water can access the cavity were detected along the trajectory. First, a fast rearrangement of MetE4 creates

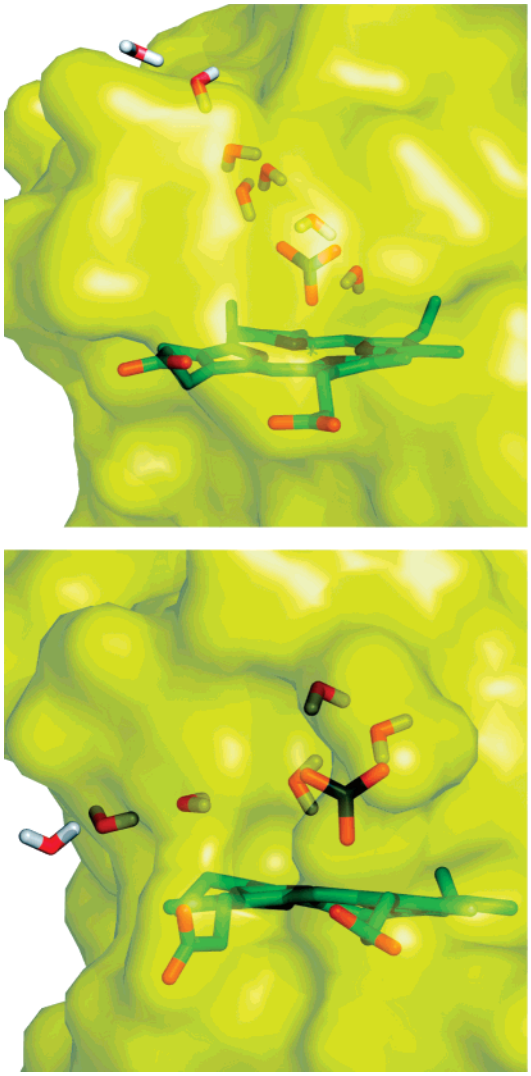

Figure 3. Representation of the pores formed in the cavity walls along the MD trajectory of the heme-bound nitrate anion. For the sake of clarity, protein residues have been omitted.

Table 1. High/low Spin Energy Gap (ΔE; kcal/mol) for the Different QM/MM Models, the Fe−O(Nitrate) Bond Distance (d; Å) for the Different Hexacoordinated Reactant Models (D, W, DL, and WL) and for the Penta-coordinated Products (PR)

	LACVP*		LACV3P*	
model	ΔE	d	ΔE	d
D	5.5	2.04	1.1	2.07
W	5.3	2.20	0.6	2.24
DL	4.5	2.13	0.9	2.15
WL	4.9	2.28	−3.1	2.32
PR	−1.0		−7.2	

a pore in the cavity as the residue moves away from the nitrate anion. Water molecules can then pass between residues TyrB10, LeuB14, MetE4, and LysE8 and solvate the nitrate anion (Figure 3). This water entry pathway is closed after 7 ns due to the rearrangement of the side chains of residues PheC7 and PheCD1, which in turn opens a new pathway between the backbone of helix C and the heme group, it being detected until the end of the trajectory (Figure 3). As a result, the nitrate anion interacts with a few water molecules (between 1 and 5, with a mean

(24) Kleywegt, G. J.; Jones, T. A. *Acta Crystallogr.* **1994**, *D50*, 1178.

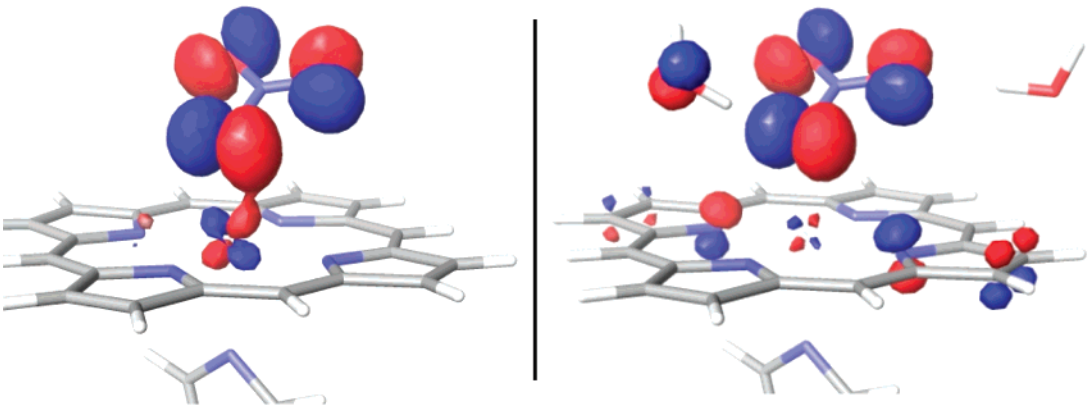

Figure 4. Molecular orbital for the iron(d_{xz})-ligand π mixing in the reduced model without (left panel) and with (right panel) two water molecules.

value of 3), which are retained around the nitrate anion during the whole simulation (see Figure S2 in the Supporting Information).

Compared to the simulations run in previous studies[12−14] for trHbN with heme-bound O_2, where the presence of water molecules in the heme cavity was a rare, transient event, it is clear that the formation of the nitrate anion triggers a relevant structural rearrangement in the heme pocket, which increases the accessibility of water molecules to the heme cavity.

QM/MM Calculations of Fe−N Bond Breaking. In order to investigate the influence of the hydrating water molecules on the breaking of the bond between the nitrate anion and the heme group, QM/MM computations were performed to determine the effect of those water molecules in the geometrical and energetic features of the nitrate protein complex formed in the last step in the NO detoxification reaction (eq 2).

$$\text{Fe}-\text{ONOO} \rightarrow \text{Fe(III)} + \text{NO}_3^- \qquad (2)$$

The starting structure for the QM/MM model was derived from a representative snapshot taken from the final part of the MD trajectory. From this snapshot, four models named dry (D), large dry (DL), wet (W), and large wet (WL) were generated. In model D all the waters in the vicinity of the nitrate anion were deleted, and the quantum region simply included the heme group, the nitrate anion, and the axial histidine. In model W the water molecules around the nitrate anion were retained and included in the QM subsystem. Finally, the QM part in models DL and WL also included TyrB10 and GlnE11, which are hydrogen-bonded to the nitrate anion. Model WL, therefore, accounts for all the direct contacts between the nitrate anion and polar groups, including water molecules (see Figure S3 in the Supporting Information).

Table 1 shows the QM/MM energy difference between the high (sextet) and low (doublet) spin states for the different models and basis set, as well as the Fe−O(nitrate) distance for the sextet spin state. The results show that hydration weakens the Fe−O bond and decreases the energy gap between high and low spin states. Thus, the Fe−O distance increases by ca. 0.17 Å when water molecules are included in the QM subsystem, and the low and high spin states become almost degenerate when the LACV3P* basis is used (see models W and D in Table 1). Interestingly, the inclusion of TyrB10 and GlnE11 in the QM subsystem (models DL and WL) leads to an additional increase in the Fe−O distance (by 0.08 Å), and the high spin state is predicted to be the ground state according to the QM-(LACV3P*)/MM computations. Table 1 also shows the energy difference for the pentacoordinated product species (PR). As expected, the ground state is the sextet spin state, which is significantly stabilized as the basis set is enlarged.

These results point out that the electrostatic screening of the nitrate anion is crucial for a correct description of the spin state and the breaking of the Fe−O bond; as for the more complete QM subsystem (model WL) the length of the Fe−O bond is increased up to 2.32 Å, and the high spin state is predicted to be the ground state. This finding can be qualitatively realized from QM calculations performed on a reduced model consisting of a capped porphyrine, an imidazole, and a nitrate anion. For this model, the B3LYP/LACV3P* energy minimization of the sextet spin state gives an Fe−O distance of 1.97 Å, which is increased 0.11 Å upon addition of two water molecules hydrogen-bonded to the nitrate anion. Inspection of Mulliken, electrostatic potential-fitted, and natural bond orbital charges indicates that the charge of the nitrate anion increases by ∼0.08 electron units upon addition of the water molecules. A molecular orbital analysis (Figure 4) indicates that the oxygen lone pairs of the nitrate anion are stabilized by the water molecules, decreasing the mixing between the iron d_{xz} and ligand π orbitals and increasing the charge transfer from the iron center to the nitrate anion (similar trends are observed for the iron(d_{z^2})−nitrate bonding orbital; see Figure S4 in the Supporting Information).

By using model WL, QM(LACV3P*)/MM computations were performed to estimate the energy profile for the breaking of the Fe−O bond in the high spin state. The reaction coordinate was defined from the Fe−O bond distance, which was enlarged by increments of ∼0.15 Å and constrained during energy minimizations. The large size of the system, about 1600 basis set functions, did not allow for more robust calculations, and the energy barrier determined by using this simple procedure must be interpreted as an upper limit. The energy barrier thus obtained amounts to ∼4 kcal/mol at an Fe−O bond distance of 3.0 Å (Figure 5), where the release of the bond distance constraint drove the system downhill to the pentacoordinated product state. For the sake of comparison, the calculation for the dry model yielded a barrier close to 18 kcal/mol.

Overall, these results point out that the increase of hydration (polarity) in the active site stabilizes the nitrate species and facilitates the breaking of the Fe−O bond in the high spin state. The hydration level, therefore, appears to be a crucial factor in controlling the stability of the nitrate-bound species.

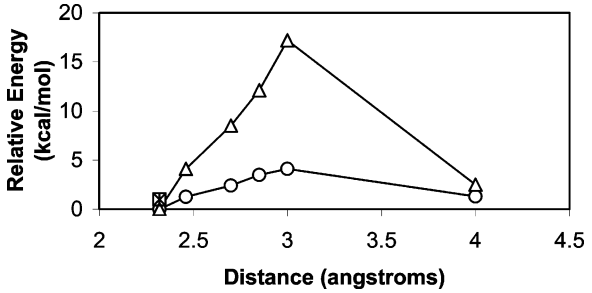

Figure 5. Energy profile (kcal/mol) obtained for the breaking of the Fe−O bond (distance in Å) for the heme-bound nitrate anion in the wet large (○) and dry (△) models.

Eggression of the Hydrated Nitrate Anion. The release of the solvated nitrate anion was examined by means of two MD simulations where the restraint imposed by the Fe−O(nitrate) bond was released. Figure 6 shows the time dependence of the distance between the heme Fe and nitrate anion for representative runs. In one case (black), the hydrated anion remains at about 6 Å from the heme iron during 2 ns due to hydrogen-bond interactions with TyrB10 and GlnE11. During the next nanosecond, it moves away passing close to MetE4 and forms a new interaction with the hydroxyl group of ThrE2. Such a position (located at around 9 Å from the heme iron) is also stabilized by interactions with the backbone amide groups of residues 47−49. After 1.5 ns, the nitrate anion leaves the protein matrix. In the other case (gray), the nitrate anion interacts with ThrE2 for 2 ns, being close to PheCD1, LeuE7, and MetE4, and then moves into the solvent through the loop formed by the backbone of residues 47 and 49 and the side chain of MetE4. Interestingly, the escape of the nitrate anion occurs in less than 5 ns in both runs, suggesting that the barrier for ligand eggression is quite low. To verify the reliability of the eggression pathway outlined above, we investigated the exit of the nitrate anion using PELE,[25] which produces a ligand random walk coupled to a side chain optimization and a minimization procedure, as an independent sampling protocol. The results fully supported the exit of the ligand toward the active site cavity defined by TyrB10, MetE4, PheCD1, and ThrE2 (see Figure S5 in the Supporting Information).

To further examine the feasibility of the nitrate eggression pathways, MSMD simulations were run to determine the free energy profile using Jarzynski's equality. By defining the reaction coordinate as the distance between the nitrate anion and the center of mass of TyrB10, in all cases the eggression of the nitrate anion followed the pathway shown in Figure 6. The resulting free energy profile (see Figure 6) shows that the transition from the heme site to the ThrE2-containing binding pocket is accompanied by a barrier of less than 1.0 kcal/mol. The interaction at the ThrE2 site corresponds to the minimum in the free energy profile, which is stabilized by about 1 kcal/mol, and the release of the anion into the solvent is accompanied by a barrier of up to 2 kcal/mol. It is interesting to note that the product release free energy barriers are similar to the barriers associated with the entry/exit of NO/O_2 through the hydrophobic tunnels. For example, the barrier for NO entrance along the long channel in the oxy protein is about only 1 kcal/mol, consistent with the fact that it is an almost diffusional process.[13] Our results

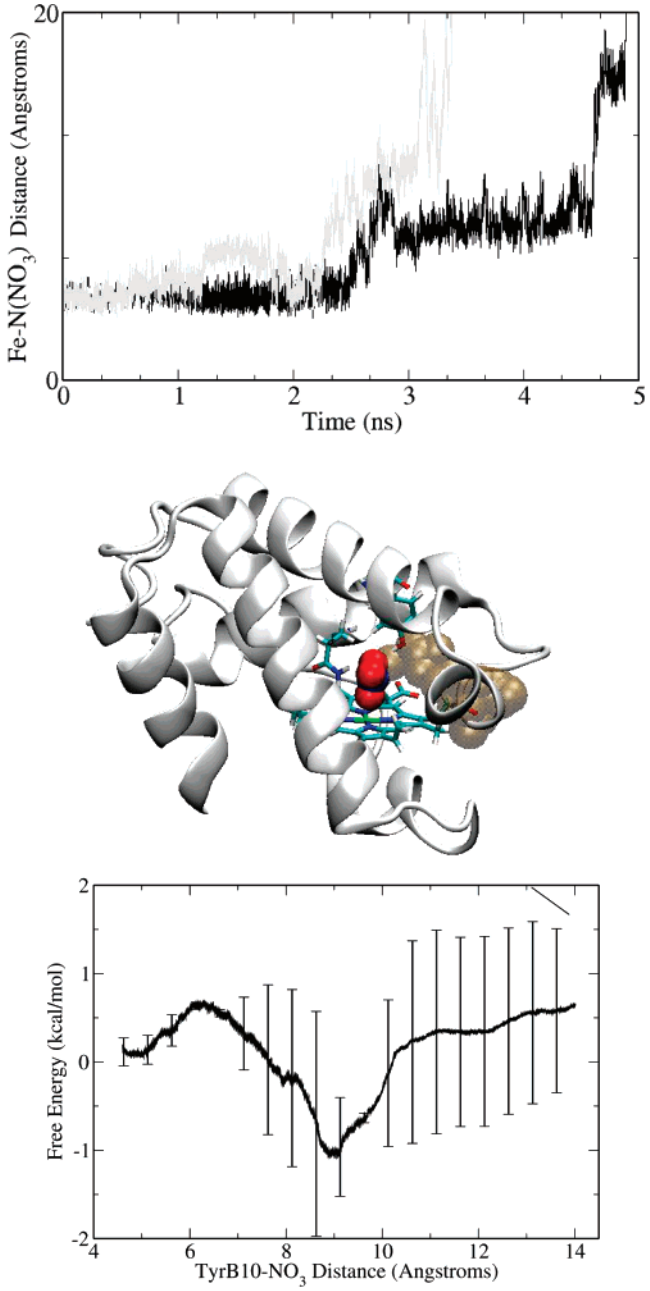

Figure 6. (Top) Time dependence of the Fe−N(nitrate) distance (Å) for two representative runs of the eggression pathways of the solvated nitrate ion in trHbN. (Middle) Representative eggression pathway of the solvated nitrate anion in trHbN. The heme group and TyrB10 are shown as sticks. The eggression pathways are shown in dark yellow. (Bottom) Free energy profile obtained for the release of nitrate anion (mean value and standard deviation derived from two different sets of MSMD runs are shown).

also suggest that ThrE2, which plays a key role in assisting the nitrate exit, may be an interesting target for site directed mutagenesis studies.

Functional Implications. The preceding results show that the overall barrier for eggression of the nitrate anion is small, as expected from the previous MD simulations performed for trHbN after having eliminated the bond restraint between the heme Fe atom and the nitrate anion. Accordingly, it can be concluded that the nitrate anion is released efficiently into the solvent once the Fe−O bond is broken. In contrast to the pathways followed by O_2 and NO to access the heme cavity, which are well-defined in the X-ray crystallographic structure

(25) Borrelli, K. W.; Vitalis, A.; Alcantara, R.; Guallar, V. *J. Chem. Theory Comput.* **2005**, 1, 1304.

of trHbN,[10] the eggression pathway of the nitrate anion is not uniquely defined, as noted in the dispersion of free energy values obtained in MSMD simulations (see Figure 6). Clearly, this finding can be explained by the difference between the narrow, well delineated branches of the protein matrix tunnel involved for migration of diatomic ligands[8] and the broader pathway followed by the nitrate anion.

The crucial event in triggering the release of the nitrate anion can be attributed to the entry of water molecules to the heme cavity, which is facilitated by the structural destabilization of the cavity walls promoted by the formation of the nitrate anion. Among other residues, such a structural destabilization affects PheCD1, which has been identified as a heme-solvent shielding residue.[9] In contrast to the *dry* environment of the heme cavity observed in the MD simulations of the wild type trHbN in both deoxygenated and oxygenated forms,[12,13] those water molecules are retained along the simulation of trHbN with the heme−Fe(III)−NO_3^- complex due to the favorable electrostatic interactions with the negative charge of the anion.

The *wet* environment created by the presence of few water molecules has a decisive contribution to the weakening of the bond between the heme Fe atom and the nitrate anion. This is reflected in the enlargement of the Fe−O distance from a value of 1.97 Å for a simple *gas-phase-like* model to 2.32 Å for the QM/MM model of the complex in trHbN (see above). Furthermore, the small energy barrier obtained for the high spin state of the heme−Fe(III)−NO_3^- complex suggests that the breaking of the Fe−O bond should be thermally feasible, which is in agreement with the known difficulties in experimentally characterizing the heme-bound nitrate anion complex.

Overall, the results point out that trHbN is able to rapidly release the nitrate anion through an eggression pathway different than that used by the diatomic ligands O_2 and NO. Thus, previous studies[13] suggest that O_2 would access the heme cavity through the short branch of the tunnel with an associated barrier of ∼4 kcal/mol, whereas migration of NO to the heme activity would take place through the long tunnel branch facilitated by the opening of the PheE15 gate upon binding of O_2 to the heme. The efficiency of the release of the nitrate anion is physiologically relevant, as it contributes to guarantee the survival of the microorganism, since it facilitates the turnover of trHbN with the concomitant uploading of O_2, and agrees with the experimental evidence that the rate of the NO detoxification is mainly limited by the access of the ligands to the heme cavity.

Conclusions

The results presented here permit us to reconcile the migration of the ligands O_2 and NO through the highly hydrophobic branches of the protein tunnel with the larger size and charged nature of the nitrate anion, as the product of the reaction leaves the enzyme using a different pathway. The migration of the nitrate anion is promoted by the increase in the hydration of the heme binding site, which contributes to the weakening of the Fe−O bond and facilitates the transition to the high spin state. In turn, the results also show that entry of the water molecules to the heme binding site is related to the structural distortion of the cavity walls induced upon formation of the product (i.e., the nitrate anion), which gives rise to the formation of different pores that allow the entrance of water molecules.

These findings complement previous experimental[4−6,8−11] and theoretical[12−14] work on the NO detoxification mechanism by trHbN from *M. tuberculosis*. Taken together, this information permits identifying certain residues that play a crucial role in the NO-dioxygenase activity of trHbN, such as PheE15, which acts as the gate of the long tunnel branch, the pair TyrB10-GlnE11, which not only modulates the O_2 binding affinity and the correct positioning of NO in the heme-bound O_2 cavity but also contributes to facilitating the opening of the gate by combining both local and global conformational changes, and ThrE2, which assists the nitrate anion along the eggression pathway. The knowledge gained from the detailed analysis of these results should be valuable to suggest possible mutations, which should affect the efficiency of the NO-detoxification mechanism by trHbN, to explain the differences in activity between related truncated hemoglobins and eventually to provide a basis for the design of a pharmacological strategy against tuberculosis based on the definition of trHbN as a potential therapeutic target.

Acknowledgment. This work was supported by grants from the ANPCYT (National Science Agency of Argentina), CONICET, and University of Buenos Aires to D.A.E, from the Spanish Ministerio de Educación y Ciencia to F.J.L. (Grant CTQ2005-08797-C02-01/BQU) and V.G. (Grant CTQ2006-10262). Calculations were performed in the *Marenostrum* Supercomputer at the Barcelona Supercomputer Center. M.A.M. thanks CONICET for a doctoral fellowship. We thank Dr. S. Kalko for a valuable discussion of the manuscript.

Supporting Information Available: Complementary figures are available free of charge via the Internet at http://pubs.acs.org.

JA076853+